Title	Fourier transform spectroscopy and cross section measurements of the Herzberg III bands of O2 at 295 K
Author(s)	Yoshino, K; Esmond, JR; Parkinson, WH; Thorne, AP; Learner, RCM; Cox, G; Cheung, ASC
Citation	Journal Of Chemical Physics, 2000, v. 112 n. 22, p. 9791-9801
Issued Date	2000
URL	http://hdl.handle.net/10722/42029
Rights	Journal of Chemical Physics. Copyright © American Institute of Physics.

Fourier transform spectroscopy and cross section measurements of the Herzberg III bands of O_2 at 295 K

K. Yoshino,[a] J. R. Esmond, and W. H. Parkinson
Harvard-Smithsonian Center for Astrophysics, 60 Garden Street, Cambridge, Massachusetts 02138

A. P. Thorne, R. C. M. Learner, and G. Cox
Blackett Laboratory, Imperial College of Science, Technology, and Medicine, London SW7 2BZ, United Kingdom

A. S.-C. Cheung
The University of Hong Kong, Hong Kong

(Received 16 November 1999; accepted 8 March 2000)

Fourier transform spectroscopic measurements of the absorption bands of the Herzberg III ($A'\,^3\Delta_u - X\,^3\Sigma_g^-$) of O_2 at 295 K have been made with a resolution of 0.06 cm^{-1} in the wavelength region 240 to 275 nm. Rotational line positions are determined with an accuracy of 0.005 cm^{-1}, and rotational term values are presented for the vibrational levels, $v'=4-11$. Precise band oscillator strengths of the (4,0)–(11,0) bands are obtained for the first time by direct measurement by summing the cross sections of individual rotational lines of the bands. The rotational line strengths and the branching ratios are also presented for the same bands. The continuity relationship for the band oscillator strengths to photodissociation continuum cross sections has been applied to the three-band systems. © *2000 American Institute of Physics.* [S0021-9606(00)01221-6]

I. INTRODUCTION

In the wavelength region above 205 nm, oxygen molecules absorb solar radiation in the Herzberg continuum of O_2, resulting in dissociation of oxygen molecules into $O(^3P)$ atoms and subsequently the production of O_3. In this wavelength region it is the absorption by O_2 and O_3 that controls the depth of penetration of solar radiation into the atmosphere, where it is available to dissociate important trace species. Three systems, Herzberg I, II, and III, contribute to the Herzberg continuum, and their individual contributions cannot be separated experimentally. Estimates of the relative cross sections of these transitions at any temperature can be obtained only by theoretical approaches[1] from known transition moments and potential curves of those states.

The $A'\,^3\Delta_u - X\,^3\Sigma_g^-$ bands of O_2 were first identified by Herzberg,[2] who observed two subbands of the (6,0) and one of the (5,0) bands. Coquart and Ramsay[3] extended observation of the $A'-X$ system for the all subbands of $v'=5-11$, and two subbands of $v'=2-5$, and accurate molecular constants were derived. Recently observations of the Herzberg III bands were extended to $v'=12$ and 13 by Slanger *et al.*[4] by using the technique of cavity ring-down spectroscopy. Bates[5] calculated transition probabilities for the Herzberg III system. Kerr and Watson[6] presented rotational line strengths of the Herzberg III system to compare with unpublished photographic work based on Coquart and Ramsay.[3] However, Kerr and Watson recommended more theoretical and experimental work in order to understand the values of the transition moment parameters. Emission bands of the $A'-X$ and $A'-a$ systems have been observed in the laboratory and also in the night-glow.[7–10]

The Herzberg bands of the three systems consist of many sharp rotational structures. These had not been measured with sufficient resolution prior to our recent work on the Herzberg I and II bands.[11–13] We used a Fourier transform (FT) spectrometer in combination with a White cell, both located at Imperial College (IC), to obtain the Doppler limited absorption spectra of the $A(v)-X(0)$ bands with $v'=4-11$ and the $c(v)-X(0)$ bands with $v'=6-16$. The intensities of the lines of the Herzberg III bands are similar to those of the Herzberg II bands, but are much lower than those of the Herzberg I bands. In this paper, we report the results of wave number measurements of the absorption bands of the $A'(v)-X(0)$ bands with $v=4-11$, made with resolution of 0.06 cm^{-1} ($R=660\,000$), again using the FT spectrometer and White cell at IC. The rotational line positions of the $A'-X$ bands, the vibronic term values of the $A'(v)$ levels, and the band oscillator strengths of the $A'-X$ system from the sum of the strengths of the individual rotational lines are reported.

II. EXPERIMENTAL PROCEDURE

The experimental setup is exactly the same as that presented in an earlier paper[13] where the experimental details are given. The total column density of O_2 was 3.26×10^{23} cm^{-2} at 800 Torr, obtained from 24 double passes of the White cell giving a total path length of almost 122 m. Absorption cross sections were obtained by using Beer's law with observed optical depths, $\ln(I_0(\lambda)/I(\lambda))$, and the known column density. We estimated the background intensity, I_0, from the regions between the absorption lines in the trans-

[a]Electronic mail: kyoshino@cfa.harvard.edu

TABLE IA. Wave numbers of the $\Omega=1$ subbands of the Herzberg III system of O_2.

N	${}^{S}R_{31}(N)$	${}^{R}R_{32}(N)$	${}^{R}Q_{31}(N)$	${}^{Q}Q_{32}(N)$	${}^{Q}P_{31}(N)$	${}^{P}Q_{33}(N)$	${}^{P}P_{32}(N)$	${}^{O}P_{33}(N)$	${}^{Q}R_{33}(N)$
					$A_1'(4)-X(0)$ band				
7	37 498.851	37 481.480C	37 483.492						
9	37 485.356C	37 464.812C	37 466.853	37 447.979C	37 450.019C	37 434.569C	37 432.623C		37 449.925C
11				37 422.979C	37 425.040C	37 406.397C	37 404.475C	37 389.564C	37 424.901C
13								37 353.071C	
					$A_1'(5)-X(0)$ band				
1	38 164.644								
3	38 165.199	38 155.006C	38 156.939	38 148.392C	38 150.341C				38 150.476C
5	38 160.772	38 147.228C	38 149.229	38 137.370C	38 139.355	38 131.156	38 129.131C	38 124.529C	38 139.382C
7	38 151.377	38 134.584C	38 136.590	38 121.415C	38 123.415	38 111.818	38 109.859C	38 101.975C	38 123.389C
9	38 137.075	38 116.968C	38 119.006	38 100.503C	38 102.531	38 087.679	38 085.727C	38 074.504C	38 102.449C
11	38 117.869	38 094.427C	38 096.486	38 074.609	38 076.762	38 058.553C	38 056.631C	38 042.088C	38 076.629C
13	38 093.696	38 066.983C	38 069.062	38 044.004C	38 046.090	38 024.519C	38 022.619C	38 004.799C	38045.904C
15	38 064.571	38 034.579C	38 036.677	38 008.350C	38 010.452C	37 985.596C	37 983.716C	37 962.617C	38 010.230C
17				37 967.760C	37 969.880C	37 941.728C	37 939.867C	37 915.499C	37 969.621C
19								37 863.460C	
					$A_1'(6)-X(0)$ band				
1	38 777.508C		38 772.664B		38 769.567B				
3	38 777.554C	38 767.618C	38 769.567C	38 761.330C	38 763.204				38 763.414C
5	38 772.452	38 759.286C	38 761.271	38 749.736C	38 751.718	38 743.755	38 741.743C	38 737.467C	38 751.748C
7	38 762.194	38 745.811C	38 747.836	38 733.069C	38 735.058	38 723.893	38 721.917C	38 714.341C	38 735.043C
9	38 746.757		38 729.240B	38 711.297C	38 713.313	38 698.891	38 696.954C	38 686.158C	38 713.243C
11	38 726.188	38 703.501	38 705.547	38 684.384	38 686.451	38 668.785B		38 652.882C	38 686.307C
13	38 700.483	38 674.563C	38 676.645B	38 652.315	38 654.397	38 633.586C	38 631.686C	38 614.477C	38 654.216C
15		38 640.521C	38 642.623	38 615.134C	38 617.236C			38 570.929C	38 617.014C
17	38 633.507B	38 601.290C	38 603.410			38 547.670C	38 545.809C	38 522.283C	
19						38 496.989C	38 495.148C		
					$A_1'(7)-X(0)$ band				
1	39 343.829	39 337.315C	39 339.191						
3	39 343.283	39 333.676C	39 335.630	39 327.578C	39 329.528	39 325.023C	39 322.939C		39 329.662C
5	39 337.395	39 324.688C	39 326.668	39 315.476C	39 317.480	39 309.807	39 307.801C	39 303.715C	39 317.488C
7	39 326.110	39 310.312C	39 312.321	39 298.032C	39 300.042	39 289.301	39 287.319C	39 280.081C	39 300.006C
9	39 309.429	39 290.549C	39 292.584	39 275.206	39 277.259	39 263.407	39 261.455C	39 251.121C	39 277.167C
11	39 287.336	39 265.387C	39 267.470	39 247.058	39 249.110	39 232.137	39 230.212C	39 216.806C	39 248.975C
13	39 259.859		39 236.987B	39 213.461C	39 215.536	39 195.456	39 193.579C	39 177.145C	39 215.361C
15	39 226.920	39 198.925B	39 201.027B	39 174.506	39 176.587	39 153.518B		39 132.074C	39 176.381C
17	39 188.550			39 130.107C	39 132.227C	39 106.074B		39 081.650C	39 131.968C
19				39 080.288C	39 082.427C				39 082.129C
					$A_1'(8)-X(0)$ band				
1	39 857.402C	39 851.056C	39 852.932		39 850.078B				
3	39 856.227	39 846.939C	39 848.897	39 841.149C	39 843.098	39 838.764C	39 836.680C		39 843.233C
5	39 849.414	39 837.182C	39 839.157	39 828.402C	39 830.388	39 823.066	39 821.064C	39 817.286C	39 830.414C
7	39 836.901	39 821.711C	39 823.766	39 810.043C	39 812.044	39 801.799	39 799.813C	39 793.007C	39 812.017C
9	39 818.744	39 800.651	39 802.677	39 786.024C	39 788.060	39 774.839C	39 772.893C	39 763.132C	39 787.970C
11	39 794.864	39 773.867C	39 775.928	39 756.356	39 758.39 7	39 742.229C	39 740.307C	39 727.609C	39 758.275C
13	39 765.227B	39 741.382C	39 743.464	39 720.974C	39 723.035	39 703.959C	39 702.059C	39 686.445C	39 722.874C
15	39 729.931	39 703.169C	39 705.270		39 681.931B	39 659.995C	39 658.115C	39 639.587C	
17	39 688.789B	39 659.261C	39 661.381	39 633.118C	39 635.238C	39 610.318C	39 608.457C		39 634.979C
19	39 641.944C	39 609.482C	39 611.620		39 582.749B	39 554.961C	39 553.119C	39 528.818C	
21		39 554.027C	39 556.184	39 522.249C	39 524.406	39 493.750C	39 491.926C		39 524.073C
23						39 426.884C	39 425.078C	39 641.646C	
					$A_1'(9)-X(0)$ band				
1	40 310.321		40 306.161B						
3	40 308.378	40 299.601C	40 301.555C	40 294.077C	40 296.058				40 296.161C
5	40 300.481	40 288.873C	40 290.859C	40 280.591C	40 282.584	40 275.743	40 273.726C	40 270.214C	40 282.603C
7	40 286.499C	40 272.129C	40 274.138	40 261.113C	40 263.133	40 253.476	40 251.504C	40 245.231	40 263.087C
9	40 266.564	40 249.392C	40 251.455	40 235.626C	40 237.670	40 225.217	40 223.272C	40 214.186	40 237.572C
11	40 240.570	40 220.631C	40 222.697	40 204.166C	40 206.212	40 190.965	40 189.055C	40 177.211C	40 206.088C
13	40 208.403	40 185.800C	40 187.886	40 166.662C	40 168.731	40 150.723C	40 148.823C	40 134.258C	40 168.562C
15	40 170.134			40 123.040C	40 125.117	40 104.413C	40 102.533C	40 085.275C	40 124.923C
17		40 097.848C	40 099.997	40 073.344C	40 075.464C			40 030.192C	40 075.205C
19						39 993.547C	39 991.706C	39 969.044C	

TABLE IA. (*Continued.*)

N	$^{S}R_{31}(N)$	$^{R}R_{32}(N)$	$^{R}Q_{31}(N)$	$^{Q}Q_{32}(N)$	$^{Q}P_{31}(N)$	$^{P}Q_{33}(N)$	$^{P}P_{32}(N)$	$^{O}P_{33}(N)$	$^{Q}R_{33}(N)$
				$A_1'(10)-X(0)$ band					
3	40 681.585C	40 681.585C	40 683.534						
5		40 669.776C	40 671.764	40 662.106C	40 664.094	40 657.722C	40 655.710C		40 664.118C
7	40 664.846	40 651.428C	40 653.444			40 634.381C	40 632.407C	40 626.711C	
9	40 642.588		40 628.740B	40 613.838	40 615.954	40 604.517C	40 602.571C		40 615.854C
11	40 613.793C	40 595.362C	40 597.423	40 580.209C	40 582.267			40 555.493C	40 582.131C
13		40 557.550C	40 559.631	40 539.924	40 542.006C	40 525.454C	40 523.554C	40 510.301C	40 541.824C
15						40 476.163C	40 474.283C	40 458.537C	
				$A_1'(11)-X(0)$ band					
7		40 947.883C	40 949.899						
9		40 920.482C	40 922.522			40 900.972C	40 899.026C		
11		40 885.841C	40 887.902			40 862.067C	40 860.145C		
13						40 815.933C	40 814.033C		

C: Line positions are calculated from the term values.
B: Lines are blended, and line positions are not available from the term values.

mission spectrum, as shown in Fig. 1 of an earlier paper.[13] The signal-to-noise ratio for I_0 was typically about 200 for the highest background intensity.

III. RESULTS AND DISCUSSION

The absorption lines were fitted to Voigt profiles by using the spectral reduction routine GREMRIC.[14] The fitting procedure provides line positions, line widths, and integrated optical depths. The wave number scale of the FT spectrometer is determined to the first order by a He–Ne laser that controls the sampling of the interferogram. It is accurately linear but requires at least one reference wave number for absolute calibration. We used the positions of the weaker lines (high N lines) of the Herzberg I bands from our previous measurements as calibration standards. At wavelengths below 250 nm the background intensity falls sharply because of the drop in reflectance of the mirrors of the White cell. Our measurements were therefore limited by wavelength region as well as by the column density, and we were not able to observe the extended high vibrational levels observed by Slanger *et al.*[4]

A. Spectroscopy of the $A'(v')-X(0)$ band

The energy-level diagram for the $A'-X$ transition has been given in earlier papers.[2,3] In an $A'\,^3\Delta_u-X\,^3\Sigma_g^-$ transition, we expect three subbands with 27 branches. Our observed line positions are presented for the three subbands ($\Omega=1-3$) in Tables IA–IC. The number of directly observed lines was limited by the weakness of the absorption at the column density used and by blends with strong lines of the Herzberg I bands as well as lines of the Herzberg II bands. The majority of directly observed lines are in the following branches: $^{S}R_{31}$, $^{Q}P_{31}$, $^{R}Q_{31}$, and $^{P}Q_{33}$ branches for $A_1'-X$; $^{S}R_{21}$, $^{Q}Q_{22}$, $^{Q}P_{21}$, $^{R}R_{21}$, and $^{R}Q_{21}$ branches for $A_2'-X$; and $^{S}R_{11}$, $^{Q}Q_{12}$, $^{R}R_{12}$, and $^{P}Q_{11}$ branches for $A_3'-X$ bands. The positions of lines that are too weak to observe directly or that are blended have been calculated from the accurate term values derived below and are marked with ''C'' in Table I. Lines followed by ''B'' are blended, and their position cannot be obtained from the term values. A portion of the $A_1'(8)-X(0)$ band is shown in Fig. 1 with rotational assignments. The groups of strong lines around 39 765 and 39 830 cm^{-1} are the $N=23$ and $N=21$ lines of the (8,0) band of the Herzberg I system.[11] The lines marked A and c belong to the $A-X$ and $c-X$ transitions, respectively. We confirmed most assignments of lines by Coquart and Ramsay.[3] All the observed wave numbers were compared with those of Coquart and Ramsay (CR) except for lines blended in either set of measurements. Differences in wave numbers (ours - CR) are plotted in Fig. 2. A slight upward shift was also observed in differences of the $c-X$ bands.[13] Similarly the bands below 38 000 cm^{-1} are shifted as observed in the (6,0) and (7,0) bands of the $c-X$ system.[13] The scatter in wave number differences (around 0.04 cm^{-1}) is very close to the estimated uncertainty, 0.03 cm^{-1} of Coquart and Ramsay.

The rotational term values of the $A'(v)$ levels can be

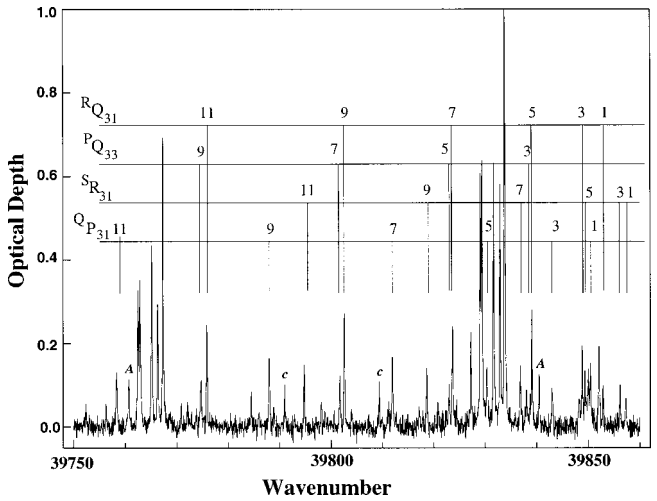

FIG. 1. The band head area of the (8,0) band. Groups of the strong lines at 39 830 and 39 765 cm^{-1} are $N=21$ and 23 lines of the $A(8)-X(0)$ bands, respectively. Lines with A and c belong to the $A-X$ and $c-X$ bands, respectively.

obtained by adding term values of the $X(0)$ levels to the observed wave numbers. The term values of the $X(0)$ level based from $N=J=0$ are calculated from molecular constants by Rouillé *et al.*,[15] which agree with those of Amiot and Verges[16] within our accuracy. The term values of the $A_1'(v)$ and $A_2'(v)$ levels with $v=5-10$ derived from our measurements are given in Table II with the uncertainty of the average. A value without an uncertainty means a single measurement. Only a few term values are given for $v=4$ and 11 and for the $A_3'(v)$ levels.

The molecular Hamiltonian for a $^3\Delta$ state in case (a) has been discussed by various authors,[17,18] and we have used the

TABLE IB. Wave numbers of the $\Omega=2$ subbands of the Herzberg III system of O_2.

N	$^SR_{21}(N)$	$^RR_{22}(N)$	$^RQ_{21}(N)$	$^QQ_{22}(N)$	$^QP_{21}(N)$	$^PQ_{23}(N)$	$^PP_{22}(N)$	$^OP_{23}(N)$	$^QR_{23}(N)$
				$A_2'(4)-X(0)$ band					
7		37 331.673C	37 333.681						
9			37 316.522B			37 284.762C	37 282.816C		
11	37 316.522B								
				$A_2'(5)-X(0)$ band					
1	38 016.833	38 010.103	38 011.981C						
3	38 017.219	38 007.169	38 009.039	38 000.622	38 002.554C	37 997.813C	37 995.729C		38 002.688C
5	38 012.566	37 999.178C	38 001.162	37 989.401	37 991.384	37 983.273C	37 981.261C	37 976.741C	37 991.411C
7	38 002.905	37 986.245	37 988.259B	37 973.222	37 975.223	37 963.783C	37 961.809C	37 954.004C	37 975.187C
9	37 988.256C	37 968.303	37 970.348	37 952.033C	37 954.073C	37 939.330C	37 937.384C	37 926.302C	37 953.979C
11	37 968.589	37 945.406	37 947.465	37 925.863	37 928.021C	37 909.893C	37 907.971C	37 893.618C	37 927.801C
13	37 943.960	37 917.506C	37 919.595	37 894.721C	37 896.803C	37 875.500C	37 873.600C	37 855.971C	37 896.642C
15				37 858.603C	37 860.705C	37 836.119C	37 834.239C	37 813.355C	37 860.483C
17								37 765.752C	
				$A_2'(6)-X(0)$ band					
1	38 631.584B	38 625.037	38 626.914C						
3	38 631.553C	38 621.706	38 623.676	38 615.411B	38 617.252B	38 610.661C	38 612.610C		
5	38 626.231	38 613.201	38 615.167	38 603.734	38 605.712	38 597.854C	38 595.842C		38 605.741C
7	38 615.705	38 599.508	38 601.496	38 586.861	38 588.881	38 577.787C	38 575.813C	38 568.334C	38 588.840C
9	38 599.966	38 580.584	38 582.634	38 564.833	38 566.846	38 552.583C	38 550.637C	38 539.955C	38 566.770C
11	38 579.022	38 556.539	38 558.546	38 537.596	38 539.656	38 522.174C	38 520.252C	38 506.409C	38 539.515C
13	38 552.851			38 505.150	38 507.243	38 486.604C	38 484.704C	38 467.685C	38 507.055C
15	38 521.459	38 492.662C	38 494.763	38 467.530	38 469.609			38 423.768C	38 469.394C
17	38 484.820	38 452.909C	38 455.029	38 424.639	38 426.768	38 399.811C	38 397.950C	38 374.663C	38 426.506C
19	38 442.876	38 407.907C	38 410.045	38 376.558C	38 378.697C	38 348.608C	38 346.767C	38 320.345C	38 378.400C
21		38 357.666C	38 359.823	38 323.182C	38 325.340C	38 292.175C	38 290.351C	38 260.826C	38 325.006C
23		38 302.162C	38 304.337			38 230.523C	38 228.717C	38 196.039C	
25						38 163.627C	38 161.840C		
				$A_2'(7)-X(0)$ band					
1	39 200.503	39 194.010B							
3	39 199.897	39 190.330	39 192.297	39 184.282	39 186.216C				39 186.351C
5	39 193.786	39 181.191	39 183.169	39 172.065	39 174.065	39 166.464C	39 164.427	39 160.404C	39 174.084C
7	39 182.284	39 166.584	39 168.613	39 154.451	39 156.461	39 145.791C	39 143.817C	39 136.677C	39 156.416C
9	39 165.313	39 146.627	39 148.633	39 131.412	39 133.452C	39 119.679C	39 117.732	39 107.531C	39 133.358C
11	39 142.900	39 121.126C	39 123.193	39 102.943	39 105.032	39 088.195C	39 086.273C	39 072.997C	39 104.872C
13	39 115.011	39 090.234	39 092.316C	39 069.021	39 071.121	39 051.218C	39 049.311	39 033.042C	39 070.931C
15	39 081.645	39 053.860C	39 055.961	39 029.642	39 031.752	39 008.847C	39 006.967C	38 987.644C	39 031.532C
17	39 042.773	39 012.017C	39 014.137	38 984.832C	38 986.970	38 961.009C	38 959.148C	38 936.801C	38 986.702C
19	38 998.417	38 964.692C	38 966.830	38 934.511C	38 936.650C	38 907.717C	38 905.875C	38 880.541C	38 936.353C
21				38 878.726C	38 880.887	38 848.960C	38 847.136C	38 818.779C	38 880.550C
23								38 751.583C	
				$A_2'(8)-X(0)$ band					
1	39 717.528	39 711.295	39 713.172C						
3	39 716.305	39 707.074	39 709.023C	39 701.266	39 703.272	39 699.003C	39 696.919C		39 703.372C
5	39 709.334	39 697.211	39 699.174	39 688.481C	39 690.469C	39 683.211C	39 681.199C	39 677.425C	39 690.493C
7	39 696.654	39 681.594	39 683.587	39 669.979C	39 671.996	39 661.804C	39 659.830C	39 653.086C	39 671.953C
9	39 678.248	39 660.268	39 662.285	39 645.781	39 647.821C	39 634.672C	39 632.726C	39 623.068C	39 647.727C
11	39 654.088	39 633.217	39 635.278C	39 615.841	39 617.911	39 601.842C	39 599.920C	39 587.366C	39 617.776C
13	39 624.172C	39 600.429	39 602.529	39 580.224	39 582.281	39 563.309C	39 561.409C	39 545.946C	39 582.114C
15	39 588.508	39 561.919C	39 564.020	39 538.808	39 540.939	39 519.052C	39 517.172C	39 498.827C	39 540.703C
17	39 547.049			39 491.711	39 493.806	39 469.068C	39 467.207C	39 445.972C	39 493.559C
19	39 499.751	39 467.499C	39 469.637	39 438.761	39 440.903			39 387.398C	39 440.613C
21				39 380.059C	39 382.218	39 351.767C	39 349.943C	39 323.039C	39 381.883C
23								39 252.916C	

TABLE IB. (*Continued*.)

N	$^{S}R_{21}(N)$	$^{R}R_{22}(N)$	$^{R}Q_{21}(N)$	$^{Q}Q_{22}(N)$	$^{Q}P_{21}(N)$	$^{P}Q_{23}(N)$	$^{P}P_{22}(N)$	$^{O}P_{23}(N)$	$^{Q}R_{23}(N)$
				$A_2'(9)-X(0)$ band					
1	40 175.183B	40 169.298C	40 171.175						
3	40 173.305	40 164.502	40 166.451C			40 157.006C	40 154.922C		
5		40 153.709	40 155.665	40 145.486	40 147.447C	40 140.632C	40 138.620C		40 147.471C
7	40 151.180	40 136.861	40 138.881			40 118.287C	40 116.319	40 110.064C	
9	40 131.018C	40 113.962	40 116.006	40 100.310	40 102.345C	40 089.918C	40 087.961		40 102.251C
11	40 104.786C	40 084.993	40 087.046C	40 068.645	40 070.708	40 055.547C	40 053.625C	40 041.890C	40 070.563C
13	40 072.461C	40 050.002	40 052.061	40 030.938	40 032.990	40 015.077C	40 013.177C	39 998.733C	40 032.817C
15	40 033.969C	40 008.815C	40 010.926	39 987.136C	39 989.237	39 968.605C	39 966.725C	39 949.530C	39 988.992C
17		39 961.518C	39 963.642	39 937.155	39 939.280	39 915.964C	39 914.103C	39 894.261C	39 939.016C
19						39 857.217C	39 855.376C	39 832.855C	
				$A_2'(10)-X(0)$ band					
3	40 561.585C	40 553.233	40 555.183C						
5	40 552.230C	40 541.362	40 543.350C	40 533.750	40 535.760	40 529.370C	40 527.358C		40 535.773C
7	40 536.420	40 523.004C	40 525.020	40 512.873	40 514.889C	40 505.967C	40 503.993C	40 498.366C	40 514.847C
9	40 514.039	40 498.163	40 500.194	40 485.547C	40 487.587C	40 476.093C	40 474.147C	40 465.962C	40 487.493C
11	40 485.208C	40 466.787	40 468.855	40 451.680	40 453.732C	40 439.744C	40 437.822C	40 427.132C	40 453.593C
13	40 449.837C	40 428.977	40 431.024	40 411.339C	40 413.421	40 396.883C	40 394.983C	40 381.763C	40 413.239C
15	40 407.834	40 384.486C	40 386.587	40 364.465	40 366.611	40 347.573C	40 345.693C	40 329.952C	40 366.368C
17		40 333.408C	40 335.528	40 310.944	40 313.149	40 291.635C	40 289.774C	40 271.637C	40 312.859C
19		40 275.706C	40 277.844			40 229.107C	40 227.266C	40 206.697C	
21		40 211.215C	40 213.372			40 159.974C	40 158.150C		
23						40 084.072C	40 082.266C		
				$'A_2'(11)-X(0)$ band					
5	40 859.558C								
7	40 841.486	40 829.249	40 831.305	40 820.201	40 822.217C				40 822.175C
9	40 816.406C	40 801.924C	40 803.964	40 790.596	40 792.615	40 782.358C	40 780.412C	40 773.290C	40 792.541C
11	40 784.182	40 767.523C	40 769.584	40 754.029	40 756.090C	40 743.509C	40 741.587C	40 732.180C	40 755.951C
13	40 744.824	40 725.931	40 728.066	40 710.335C	40 712.438	40 697.615C	40 695.715C	40 684.121C	40 712.235C
15		40 677.284C	40 679.385	40 659.475C	40 661.577C	40 644.571C	40 642.691C	40 628.948C	40 661.355C
17						40 584.433C	40 582.572C	40 566.624C	

C: Line positions are calculated from the term values.
B: Lines are blended, and line positions are not available from the term values.

matrix elements tabulated in Brown *et al.*[19] for the calculation of the rotational levels. The molecular constants involved in the calculation are the band origin T_0; the rotational constants B and D; the spin-orbit constant A; spin-spin constant λ; and the spin-rotation constant γ for the $A'\,^3\Delta_u$ state. The molecular constants obtained from our least squares fit for the $v=5-10$ levels of the $A'\,^3\Delta_u$ state are listed in Table III. The rms deviations of our fits in each band are also included.

B. Photoabsorption cross sections and the band oscillator strengths of the $A'(v)-X(0)$ band

The integrated cross sections of the rotational lines of the $A'-X$ system are obtained by fitting lines with all parameters free for isolated lines. The results are presented in Table IV for the (6,0) through (11,0) bands of $A_1'-X$ and $A_2'-X$. The integrated cross sections of the blended lines are estimated by using the observed branching ratios and the rotational distribution. These are labeled in the table as A, A', and c for lines blended with $A-X$, $A'-X$, and $c-X$ bands, respectively. The cross sections in Table IV are derived from the total column density of O_2, not from the column density of the rotational levels concerned, and must be divided by the fractional populations of the rotational levels to obtain values proportional to the line oscillator strengths.

The integrated cross section of a band is obtained by

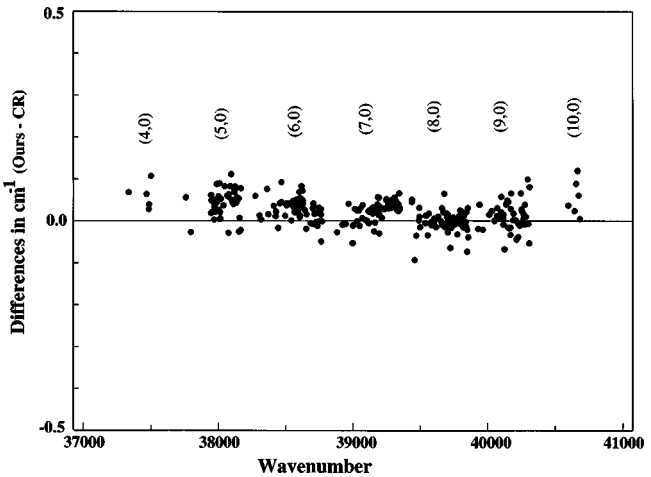

FIG. 2. Differences in the observed line positions between our results and those of Coquart and Ramsay (Ref. 3). A slight upward shift is also observed in differences in the $c-X$ bands (Ref. 13).

TABLE IC. Wave numbers of the $\Omega=3$ subbands of the Herzberg III system of O_2.

N	$^{S}R_{11}(N)$	$^{R}R_{12}(N)$	$^{R}Q_{11}(N)$	$^{Q}Q_{12}(N)$	$^{Q}P_{11}(N)$	$^{P}Q_{13}(N)$	$^{P}P_{12}(N)$	$^{O}P_{13}(N)$	$^{Q}R_{13}(N)$
					$A_3'(5)-X(0)$ band				
11			37 795.053			37 757.931			
					$A_3'(6)-X(0)$ band				
9		38 430.884	38 432.924C			38 372.469C	38 370.547C		
11									
13	38 402.097C	38 376.615B	38 378.697B						
15	38 370.249			38 316.748	38 318.850C				38 318.628C
17				38 273.447	38 275.562C			38 223.897C	38 275.303C
19								38 169.142C	
					$A_3'(7)-X(0)$ band				
9	39 018.183B	38 999.586	39 001.626C			38 941.171C	38 939.249C		
11	38 995.392								
13	38 967.176C	38 942.601C	38 944.682	38 921.528	38 923.608C	38 861.214C	38 859.334C		38 923.426C
15				38 881.827	38 883.929C			38 840.139C	38 883.707C
17								38 788.976C	
					$A_3'(8)-X(0)$ band				
11	39 510.439C	39 489.657	39 491.718C						
13		39 456.562C	39 458.644	39 436.570	39 438.652C	39 419.749C	39417.849C		39 438.470C
15	39 444.232C					39 375.175C	39 373.295C	39 355.183C	
17				39 347.418	39 349.538C				39 349.279C
19								39 243.117C	
					$A_3'(9)-X(0)$ band				
9	39 992.656C								
11				39 930.279	39 932.340C				39 932.201C
13								39 860.371C	
15									
17		39 822.434C	39 824.554						
19						39 718.134C	39 716.292C		
					$A_3'(10)-X(0)$ band				
7	40 405.083C								
9	40 382.656C			40 354.210	40 356.250C				40 356.156C
11	40 353.796C			40 320.279	40 322.340C			40 295.795C	40 322.201C
13	40 318.308C	40 297.420C	40 299.501	40 279.927	40 282.009C			40 250.371C	40 281.827C
15		40 253.037	40 255.139C	40 232.959	40 235.061C	40 216.033C	40 214.153C	40 198.540C	40 234.839C
17						40 160.186C	40 158.325C	40 140 .108	
					$A_3'(11)-X(0)$ band				
7	40 719.753C								
9				40 668.880	40 670.920C				40 670.826C
11								40 610.465C	
13		40 604.528C	40 606.609						
15	40 577.073C					40 523.141C	40 521.261C		
17				40 480.258	40 482.379C				40 482.120C
19								40 375.958C	

C: Line positions are calculated from the term values.
B: Lines are blended, and line positions are not available from the term values.

adding up the rotational line cross sections belonging to it. The results are presented in Table V under ''observed.'' The observed lines are limited in rotational quantum number to between $N=15$ and $N=23$, and the effects from the higher N lines cannot be ignored. We extended the sums to $N=29$ by using a Boltzmann distribution, and the results are presented in Table V under ''extended.'' The uncertainty in the value of the column density is negligible and the estimated error in this table comes mainly from the noise in the FT spectra, and the increased error toward the shorter wavelengths is due to the lower background intensity already referred to.

The band oscillator strengths are given by

$$f(v',v'')=\frac{mc^2}{\pi e^2}\frac{1}{\tilde{N}(v'')}\int \sigma(\nu)\,d\nu, \tag{1}$$

in which $\tilde{N}(v'')$ is the Boltzmann population of the absorb-

TABLE II. The term values of the $A'\,^3\Delta_u$ level of O_2 (cm^{-1}).

N	$v=4$	$v=5$	$v=6$	$v=7$	$v=8$	$v=9$	$v=10$	$v=11$
				$^3\Delta_{3u}(F_1)$				
	c-component							
1			38 770.565b		39 851.076b			
3		38 165.643	38 778.506	39 344.829(02)	39 858.400	40 311.328(31)		
5		38 180.496(08)	38 792.856	39 358.602(23)	39 871.528(02)	40 323.718(34)	40 705.232	
7		38 201.910(20)	38 813.564(37)	39 378.527(08)	39 890.538(21)	40 341.609(10)		
9	37 577.331	38 229.855(13)	38 840.649(34)	39 404.573(16)	39 915.376(06)	40 364.978	40 743.260(68)	
11	37 612.668	38 264.396(05)	38 874.074(05)	39 436.742(05)	39 946.042(16)	40 393.855(25)	40 769.898(04)	
13		38 305.501(02)	38 913.813(02)	39 474.958(08)	39 982.471(30)	40 428.159(50)	40 801.421	
15		38 353.114	38 959.898	39 519.265(13)	40 024.618b	40 467.804(19)		
17		38 407.236		39 569.583	40 072.594	40 512.796		
19				39 625.906	40 126.187b			
21					40 185.423			
	d-component							
2			38 773.662b	39 340.190	39 853.931	40 307.160b		
4		38 172.257(27)	38 784.869	39 350.927(08)	39 864.190(13)	40 316.857	40 698.836	
6		38 190.354(21)	38 802.412(04)	39 367.814(11)	39 880.308(18)	40 331.997	40 712.902	
8	37 561.975	38 215.079(11)	38 826.306(13)	39 390.807(09)	39 902.245	40 352.624(04)	40 731.923	41 028.378
10	37 594.164	38 246.320	38 856.552b	39 419.901(06)	39 929.996(10)	40 378.744(28)	40 756.052b	41 049.834
12		38 284.116	38 893.183(11)	39 455.076(32)	39 963.556	40 410.320	40 785.051	41 075.530
14		38 328.480	38 936.060b	39 496.379b	40 002.879	40 447.297	40 819.047	
16		38 379.343	38 985.285	39 543.658b	40 047.933			
18			39 040.766		40 098.737	40 537.324		
20					40 155.100			
22					40 217.201			
				$^3\Delta_{2u}(F_2)$				
	c-component							
3		38 017.856(25)	38 632.599b	39 201.518(23)	39 718.539(30)	40 176.182b	40 565.361b	
5		38 032.525(06)	38 646.855(07)	39 215.198(06)	39 731.607	40 188.585(05)	40 576.887(16)	
7		38 053.708(09)	38 667.361(07)	39 234.937(11)	39 750.474(02)		40 593.368	40 900.696
9		38 081.385	38 694.176(15)	39 260.764(01)	39 775.133(00)	40 229.657(07)	40 614.899	40 919.947(19)
11		38 115.568	38 727.282(04)	39 292.639(19)	39 805.543(15)	40 258.330(01)	40 641.360(13)	40 943.718
13	37 504.153b	38 156.218	38 766.652(06)	39 330.528(10)	39 841.711(13)	40 292.414(26)	40 672.836	40 971.832(31)
15		38 203.367	38 812.278(14)	39 374.416(11)	39 883.587(21)	40 331.900	40 709.252(32)	41 004.239
17			38 864.121(04)	39 424.317(13)	39 931.174(13)	40 376.634(04)	40 750.474(47)	
19			38 922.176	39 480.129	39 984.389(14)			
21			38 986.356	39 541.900(04)	40 043.233(02)			
	d-component							
2		38 012.980	38 627.912	39 196.885b	39 714.170	40 172.174		
4		38 024.387(51)	38 638.968(14)	39 207.578(23)	39 724.325	40 181.753	40 570.484	
6		38 042.304	38 656.316(15)	39 224.312(07)	39 740.325(18)	40 196.820(15)	40 584.488	
8	37 412.168	38 066.736	38 679.989(20)	39 247.085(07)	39 762.078(16)	40 217.343(26)	40 603.499	40 909.764(28)
10	37 443.837b	38 097.660(04)	38 709.941(07)	39 275.962(24)	39 789.609(16)	40 243.316(02)	40 627.511(06)	40 931.276
12		38 135.097(01)	38 746.201(38)	39 310.815(09)	39 822.906	40 274.674	40 656.480(05)	40 957.212
14		38 179.003		39 351.731	39 861.936(13)	40 311.489(23)	40 690.457(25)	40 987.455(37)
16			38 837.426	39 398.624	39 906.683	40 353.588	40 729.250	41 022.048
18			38 892.385	39 451.493		40 400.994	40 772.884	
20			38 953.525	39 510.310	40 013.117		40 821.324	
22			39 020.840				40 874.389	
24			39 094.285					
				$^3\Delta_{1u}(F_3)$				
	c-component							
9						40 483.562	40 798.232	
11			39 145.495b		40 119.968	40 509.968		
13			39 183.023(04)	39 698.067		40 541.424		
15		38 661.512	39 226.591			40 577.723		
17		38 712.918(08)		39 786.894			40 919.735	
	d-component							
10	37 945.701	38 560.236A	39 128.938	39 646.310b				
12	37 982.673			39 679.346				
14		38 638.112b	39 204.098	39 718.059		40 558.917	40 866.025	
16						40 597.801		
18					40 261.910			

b: Term values are obtained from the blended lines.

TABLE III. Molecular constants (cm^{-1}) of the $A'\,^3\Delta_u$ state of O_2

v	T_0	B	10^5D	A	λ_A	γ	rms
5	38 006.456(12)	0.815 33(14)	0.607(51)	−73.141(13)	−0.0917(61)	0.0469(82)	0.018
6	38 621.654(04)	0.790 01(04)	0.766(07)	−72.211(06)	−0.0898(34)	0.0791(29)	0.010
7	39 191.003(07)	0.760 84(08)	0.885(18)	−70.994(08)	−0.0992(39)	0.1238(39)	0.016
8	39 708.607(09)	0.726 99(09)	1.106(18)	−69.406(09)	−0.1484(48)	0.2154(51)	0.022
9	40 167.072(16)	0.686 18(24)	1.398(67)	−67.228(25)	−0.2264(13)	0.353(14)	0.032
10	40 557.298(41)	0.6360(17)	2.007(37)	−64.296(45)	−0.429(20)	0.669(34)	0.035

ing vibrational level, and the integration of the cross section $\sigma(\nu)$ is performed over all of the rotational lines belonging to the (v',v'') band. For O_2 at 295 K, $\tilde{N}(0)$ is equal to the column density N, and Eq. (2) yields the band oscillator strength of the $(v',0)$ band,

$$f(v,0)=1.130\times10^{12}\int\sigma(\nu)\,d\nu. \tag{2}$$

The band oscillator strengths, $f(v,0)$, with $v=5-11$ have been determined by Eq. (2) using the extended integrated cross sections. The results are presented in the 6th and 11th columns of Table V for the $A_1'-X$ and $A_2'-X$ bands, respectively. Huestis *et al.*[20] observed two bands of the $A'-X$ system by cavity ring-down spectroscopy. They also recommended oscillator strengths for other bands on the basis of their experimental results and the Franck–Condon factors. These are given in the fourth and fifth columns of Table VI, where our combined band oscillator strengths of the $A_1'-X$ and $A_2'-X$ bands are also presented. For comparison we give in the third column the relative band oscillator strengths obtained from the transition probabilities of Bates.[5]

C. A continuity relationship from the band oscillator strengths to photodissociation cross sections

A continuity relationship from the band oscillator strengths to photodissociation cross sections was presented by Allison and Dalgarno.[21] Saxon and Slanger[22] applied this procedure to the Schumann–Runge bands of O_2 $(v'=12-20)$. The cross section for the photodissociation continuum is related to the band oscillator strength, f, for a nearby band, by the expression[22]

$$\sigma(E)=(\pi e^2/mc^2)df_{v'v''}/d\nu=8.85\times10^{-13}f_{v'0}\rho(E). \tag{3}$$

Here, ρ (E) is given by

$$\rho(E)=\left(\frac{E(v'+1)-E(v'-1)}{2}\right)^{-1}. \tag{4}$$

For the Herzberg bands of O_2, Huestis *et al.*[20] presented the differential oscillator strengths through the dissociation limit in Fig. 6 of their paper, under the assumption that the Herzberg I continuum is 86% of the Herzberg continuum. Continuity was demonstrated with the differential oscillator strengths of Hasson *et al.*,[23] which are very close to our recent FT measurements of the Herzberg I band.[12] They compared the band oscillator strengths of the (8,0), (13,0), and (9,0) bands of the Herzberg I, II, III, respectively, and justified the assumption that 86% of the Herzberg continuum comes from the Herzberg I continuum. Their ratio for the (8,0) and (13,0) bands would be 25, which can be compared with our ratio 29.

Amoruso *et al.*[24] reported new measurements of the photoabsorption cross sections of the Herzberg continuum with values about 15% smaller than those of the previous work of Yoshino *et al.*,[25] which were based on measurements of Jenouvrier *et al.*[26,27] Amoruso *et al.* stated that the scatter of the data and the anomalous behavior for the vibrational levels above $v=7$ do not allow any definitive conclusion about the validity of the various continuum cross-section measurements that are based on the principle of continuity of oscillator-strength density. However, the band oscillator strengths of the Herzberg I bands are well determined,[28] and make a smooth connection to the continuum of Yoshino *et al.*[25] under the assumption that 86% comes from the Herzberg I continuum.

As a result of these measurements of the Herzberg III bands in combination with cross-section measurement of the Herzberg I and II bands,[12,13] we know all the band oscillator strengths of the Herzberg system, and can now demonstrate the continuity relationship without any assumption. Figure 3 presents the two measurements of the continuum[24,25] and the derived effective cross sections, $\sigma(E)$, of the Herzberg I bands (gray-filled circle). The derived effective cross sec-

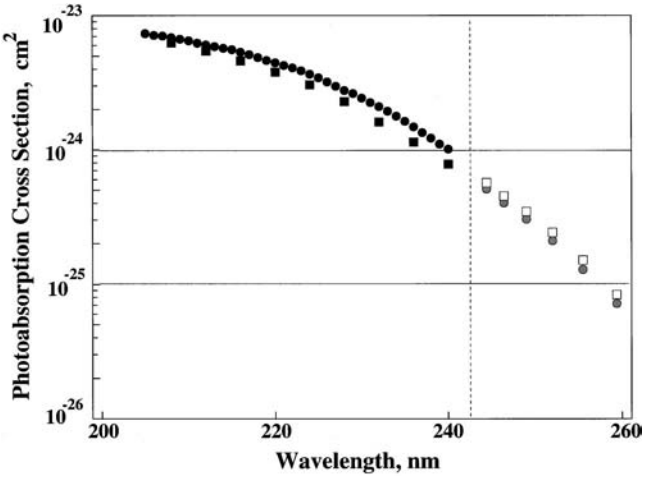

FIG. 3. The differential oscillator strengths for the Herzberg band systems and the cross sections for the Herzberg continuum. The continuum is given by filled circles by Yoshino *et al.* (Ref. 25) and filled squares by Amoruso *et al.* (Ref. 24). Values for the Herzberg I bands are given by gray filled circles (Ref. 12) and values for the combined Herzberg I, II and III bands (Ref. 13) by open squares. The dissociation limit is indicated by the broken line.

TABLE IV. Integrated cross sections of lines of the Herzberg III bands of O_2 at 295 K in units of 10^{-27} cm^2cm^{-1}.

	$A_1'(6)-X(0)$ band						$A_1'(7)-X(0)$ band					
N	$^SR_{31}$	$^RR_{32}$	$^RQ_{31}$	$^QQ_{32}$	$^QP_{31}$	$^PQ_{33}$	$^SR_{31}$	$^RR_{32}$	$^RQ_{31}$	$^QQ_{32}$	$^QP_{31}$	$^PQ_{33}$
1	25*A*′	5E	31*A*	8E	13*A*′		34	4E	46	12E	25E	
3	52*A*′	11E	62*A*′	18E	49	18*c*	62	10E	93	25E	46	34*c*
5	53*A*	15E	93	25E	59	28	74	13E	155	35E	77	49
7	68	17E	105	29E	71	34	80	15E	152	40*A*	87	49
9	56	17E	87*c*	29E	93	22	68	15	155	28	96	53
11	43	15	124	22	56	26E	65	14E	152	49	68	40
13	34	12E	71	25	37	19*A*′	62	11E	136	31	53	28
15	34E	10E	65	16E	19*A*′	16E	43	9E	90	19	56	40
17	19*A*′	7E	46	12E	27E	12E						
Total	384	109	684	184	424	175	488	91	979	239	508	293

	$A_1'(8)-X(0)$ band							$A_1'(9)-X(0)$ band					
N	$^SR_{31}$	$^RR_{32}$	$^RQ_{31}$	$^QQ_{32}$	$^QP_{31}$	$^PQ_{33}$	$^OP_{33}$	$^SR_{31}$	$^RQ_{31}$	$^QQ_{32}$	$^QP_{31}$	$^PQ_{33}$	$^OP_{33}$
1	49	8E	62	18E	42*c*			65	71	16E	31*c*		
3	80	18E	127	38E	77	53	25E	130	93c	35E	62	35E	23E
5	99	25E	158	53E	102	62	34	139	182E	48E	111	49*c*	32E
7	118	28E	195	60E	130	74	39E	147*A*	201	54E	124[a]	59	34
9	105	28	180	60E	130	74	39E	118	201	54E	130	53	36E
11	90	25E	176	37	121	71E	35E	118	189	49	105	49	34
13	86*A*	21E	161	43	102	58E	29E	90	186	41E	62	41E	27E
15	74	16E	111	34E	75*A*	56	22E	74[a]	117E	31E	40	32E	20E
17	49	11E	118	24E	46*A*′	32E	16E						
19	32E	8E	83	34	38*c*	21E	10E						
21	20E	5E	56[a]	10E	43	13E	7E						
Total	802	193	1427	411	906	514	256	881	1240	328	665	318	206

	$A_1'(10)-X(0)$ band					$A_2'(5)-X(0)$ band				
N	$^SR_{31}$	$^RQ_{31}$	$^QQ_{32}$	$^QP_{31}$	$^PQ_{33}$	$^SR_{21}$	$^RR_{22}$	$^RQ_{21}$	$^QQ_{22}$	$^QP_{21}$
1	42E	58E	24E	33E		19	31	20E		
3	91E	127	52E	71E	18E	37	31	31	19	19E
5	126E	195*c*	72E	124[a]	25E	28	31E	49	34	22
7	155[a]	202	82E	105	28E	46	28	56*A*′	37	22
9	130[a]	152*c*	77	102*c*	28*c*	49*A*′	25	71	46*c*	29*c*
11	129E	179*A*	74*A*	93	25E	53	19	77	28	37*c*
13	106E	167	65	84E	21E	49	26E	68	28E	22*A*
Total	779	1080	446	612	145	281	191	372	192	151

	$A_2'(6)-X(0)$ band					$A_2'(7)-X(0)$ band					
N	$^SR_{21}$	$^RR_{22}$	$^RQ_{21}$	$^QQ_{22}$	$^QP_{21}$	$^SR_{21}$	$^RR_{22}$	$^RQ_{21}$	$^QQ_{22}$	$^QP_{21}$	$^PP_{22}$
1	38*A*′	40	40E			56	28	52E			
3	56*A*′	53	49	43	22*A*′	80	59	65	49	34	28E
5	65	59	114	62	28	84	56	111	84	46	16
7	80	62	111	59	37	93	80	142	114	68	56
9	71	40	111	65	40	105	114	167	108[a]	82*A*	46
11	74	59	118	62	53	121	74E	176[a]	93[a]	74*A*	56
13	71	50E	102E	43	56	111	37	148	49	68	25
15	62	38E	99	37E	29E	71E	47E	124	34	59	25E
17	59	27E	68	19	34	59	34E	124[a]	38E	56	18E
19	31	18E	65	22*A*′	25*A*′	53	22E	87	25E	22E	12E
21	15E	11E	43	11E	9E	21E	14E	30E	16E	28	7E
23	9E	7E	31	6E	5E						
Total	631	464	951	429	338	854	565	1226	610	537	289

TABLE IV. (*Continued*.)

	$A_2'(8)-X(0)$ band						$A_2'(9)-X(0)$ band					
N	$^SR_{21}$	$^RR_{22}$	$^RQ_{21}$	$^QQ_{22}$	$^QP_{21}$	$^PP_{22}$	$^SR_{21}$	$^RR_{22}$	$^RQ_{21}$	$^QQ_{22}$	$^QP_{21}$	$^PP_{22}$
1	65	77	34				44*A*	29*A*	82*A*			
3	96	87	105	53	59	52*A*′	77[a]	62[a]	176E	97*A*	104E	33E
5	102	109b	161	110*A*	124	72E	132E	108[a]	186[a]	139[a]	144E	45E
7	145	115*A*	228*A*	125*A*	96	87	155[a]	124[a]	232	152*A*	164E	62
9	170[a]	105	228*A*	161[a]	155[a]	82E	186[a]	77	263	164[a]	164[a]	32
11	161	93	201[a]	102	108	74E	135E	68	266*c*	136	136[a]	46E
13	122E	53	189	99	111	61E	112E	56	235	118	124	46
15	121	66E	189	65	90	47E	62c	56E	192	87	99[a]	29E
17	62	47E	93E	46*A*′	56	28	61E	40E	161	40	68	21E
19	49	19[a]	99[a]	37	46	22E						
21	27E	19E	38E	21E	31	14E						
Total	1120	790	1565	819	876	539	964	620	1793	933	1003	314

	$A_2'(10)-X(0)$ band					$A_2'(11)-X(0)$ band				
N	$^SR_{21}$	$^RR_{22}$	$^RQ_{21}$	$^QQ_{22}$	$^QP_{21}$	$^SR_{21}$	$^RR_{22}$	$^RQ_{21}$	$^QQ_{22}$	$^QP_{21}$
1	59*A*	31E	86E			38E	43E	65E		
3	127*A*	90	105	78*A*	87*A*	83E	92E	141E	82E	92E
5	176*A*	90[a]	260E	102	90	115E	128E	195E	124	128E
7	210	104E	272	124E	136*A*	130	155[a]	195	111	146E
9	198	102	247	102	136*A*	130E	155	254[a]	133	139
11	180*A*	77	263	105	123*A*	124[a]	131E	139[a]	121	131E
13	139	74	260	124*c*	93	90	80	198	97E	114
15	114	60E	207	65	99	74E	90	145	74E	83E
17	81E	42E	155	56	71					
19	54E	28E	96	33E	37E					
21	34E	18E	71	21E	23E					
Total	1372	716	2022	810	895	784	874	1332	742	833

[a]Intensity estimated from fitting value, because of influence of strong $A-X$ features on the fit.
c: Overlap with another $c-X$ line; value estimated from measured blend.
A': Overlap with an $A'-X$ line; value estimated from measured blend.
A: Overlap with a strong $A-X$ line; value calculated using Boltzman distribution estimate.
E:. Extended values for lines not measured using Boltzman distribution estimate.

TABLE V. Integrated cross sections (units of 10^{-24} cm^2 cm^{-1}) and the band oscillator strengths f (units of 10^{-12}) of the $A_1'-X(0)$ and $A_2'-X(0)$ bands of O_2.

	$A_1'(v)-X(0)$					$A_2'(v)-X(0)$				
Band	Wavelength (nm)	Integrated cross section observed	extended	Error %	f	Wavelength (nm)	Integrated cross section observed	extended	Error %	f
5,0	262.1					263.1	1.19	1.54	8	1.74
6,0	257.9	1.96	2.15	7	2.43	258.9	2.81	2.85	6	3.22
7,0	254.2	2.60	3.05	6	3.45	255.1	4.08	4.20	6	4.75
8,0	250.9	4.51	4.64	6	5.24	251.8	5.71	5.87	5	6.63
9,0	248.1	3.64	4.27	10	4.83	248.9	5.63	6.19	6	6.99
10,0	245.8	3.06	3.97	10	4.49	246.5	5.82	5.98	10	6.76
11,0	244.0					244.7	4.57	5.36	20	6.06

TABLE VI. The band oscillator strengths f (units of 10^{-12}) of the Herzberg III bands of O_2.

Band	Present	Ba[a]	H[b]-Experimental	H[b]-FC
6,0	5.65	30.2		8.4
7,0	8.20	44.9		12.5
8,0	11.57	62.8		16.4
9,0	11.82	76.2	19.2	19.2
10,0	13.52	83.9		20.2
11,0		80.8	16.7	16.7

[a]Ba: Bates (Ref. 5), theory.
[b]H-: Huestis *et al.* (Ref. 20), experimental and theory.

tions for the the entire Herzberg system are represented by open squares. The continuum measurement by Amoruso *et al.* makes a smooth continuation to the Herzberg I bands, but not to the entire Herzberg band system. On the other hand, the continuum of Yoshino *et al.* is slightly too high to make a smooth connection to the band systems. Because we ignored the contribution of the $A_3'-X$ bands, our results here are lower limits of the Herzberg band system. The measurements of the Herzberg continuum by Amoruso *et al.* appear to be too small.

IV. CONCLUDING REMARKS

This work provides the first absorption intensity measurements of the Herzberg III bands free of problems arising from inadequate spectral resolution. However, our limited column densities of oxygen molecules limited our ability to observe all lines belonging to the Herzberg system. We cannot present any intensity measurements of the $A_3'-X$ system, which is the weakest system. Therefore the band oscillator strengths presented here are a lower limit based on our observations.

ACKNOWLEDGMENTS

This work was supported in part by NSF Division of Atmospheric Sciences Grant No. ATM-91-16562 to Harvard College Observatory, and by the NASA Upper Atmospheric Research Program under Grant No. NAG5-484 to the Smithsonian Astrophysical Observatory. We also acknowledge the Paul Instrument Fund of the Royal Society for the development of the VUV-FT spectrometer.

[1] R. P. Saxon and T. G. Slanger, J. Geophys. Res. **91D**, 9877 (1986).
[2] G. Herzberg, Can. J. Phys. **31**, 657 (1953).
[3] B. Coquart and D. A. Ramsay, Can. J. Phys. **64**, 726 (1986).
[4] T. G. Slanger, D. L. Huestis, P. C. Cosby, H. Naus, and G. Meijer, J. Chem. Phys. **105**, 9393 (1996).
[5] D. R. Bates, Planet. Space Sci. **37**, 881 (1989).
[6] C. M. L. Kerr and J. K. G. Watson, Can. J. Phys. **64**, 36 (1986).
[7] T. G. Slanger, J. Chem. Phys. **69**, 4779 (1978).
[8] T. G. Slanger, Chem. Phys. Lett. **66**, 344 (1979).
[9] T. G. Slanger and D. L. Huestis, J. Geophys. Res. **86**, 3551 (1981).
[10] T. G. Slanger and D. L. Huestis, J. Chem. Phys. **78**, 2274 (1983).
[11] K. Yoshino, J. E. Murray, J. R. Esmond, Y. Sun, W. H. Parkinson, A. P. Thorne, R. C. M. Learner, and G. Cox, Can. J. Phys. **72**, 1101 (1994).
[12] K. Yoshino, J. R. Esmond, J. E. Murray, W. H. Parkinson, A. P. Thorne, R. C. M. Learner, and G. Cox, J. Chem. Phys. **103**, 1243 (1995).
[13] K. Yoshino, J. R. Esmond, W. H. Parkinson, A. P. Thorne, R. C. M. Learner, and G. Cox, J. Chem. Phys. **111**, 2960 (1999).
[14] J. W. Brault, private communication.
[15] G. Rouillé, G. Millot, R. Saint-Loup, and H. Berger, J. Mol. Spectrosc. **154**, 372 (1992).
[16] C. Amiot and J. Verges, Can. J. Phys. **59**, 1391 (1981).
[17] J. M. Brown, E. A. Colbourn, J. G. K. Watson, and F. D. Wayne, J. Mol. Spectrosc. **74**, 294 (1979).
[18] L. Veseth, Mol. Phys. **26**, 101 (1973).
[19] J. M. Brown, A. S-C. Cheung, and A. J. Merer, J. Mol. Spectrosc. **124**, 464 (1987).
[20] D. L. Huestis, R. A. Copeland, K. Knutsen, T. G. Slanger, R. T. Jongma, M. G. H. Boogaarts, and G. Meijer, Can. J. Phys. **72**, 1109 (1994).
[21] A. C. Allison and A. Dalgarno, J. Chem. Phys. **55**, 4342 (1971).
[22] R. P. Saxon and T. G. Slanger, J. Geophys. Res. **96**, 17291 (1991).
[23] V. Hasson, R. W. Nicholls, and V. Degen, J. Phys. B **3**, 1192 (1970).
[24] A. Amoruso, L. Crescentini, M. S. Cola, and G. Fiocco, J. Quant. Spectrosc. Radiat. Transf. **56**, 145 (1996).
[25] K. Yoshino, A. S.-C. Cheung, J. R. Esmond, W. H. Parkinson, D. E. Freeman, S. L. Guberman, A. Jenouvrier, B. Coquart, and M. F. Merienne, Planet. Space Sci. **36**, 1469 (1988).
[26] A. Jenouvrier, B. Coquart, and M. F. Merienne, J. Quant. Spectrosc. Radiat. Transf. **36**, 349 (1986).
[27] A. Jenouvrier, B. Coquart, and M. F. Merienne, Planet. Space Sci. **34**, 253 (1986).
[28] K. Yoshino, D. L. Huestis, and R. W. Nicholls, J. Quant. Spectrosc. Radiat. Transf. **60**, 1091 (1998).